Schottky barrier modulation via calcium hydroxide nanoparticles on g-C_3N_4/Ti_3C_2 for overall photocatalytic applications

Zeeshan Asghar [a, b], Jawad Ahmad Jrar [a, b], Alauddin [a, b], Faheem K. Butt [c], Kewang Zheng [d], Yongcai Zhang [e], Nian-Tzu Suen [e, f*] and Jianhua Hou [a*]

[a] School of Environmental Science and Engineering, Yangzhou University, Yangzhou 225127, China.

[b] College of Physical Science and Technology, Yangzhou University, Yangzhou, 225009, China.

[c] Department of Physics, Division of Science and Technology, University of Education Lahore, 54000, Pakistan.

[d] School of Chemistry and Materials Science, Hubei Engineering University, Xiaogan 432000, Hubei, China

[e] School of Chemistry and Chemical Engineering, Yangzhou University, Yangzhou 225009, China

[f] Yunnan Key Laboratory of Electromagnetic Materials and Devices, Yunnan University, Kunming 650500, P. R. China

Corresponding Authors:

Professor Dr. Nian-Tzu Suen: 006641@yzu.edu.cn

Professor Dr. Jianhua Hou: jhhou@yzu.edu.cn

Experimental Methods

The chemicals used include Ti_3AlC_2 >98% (Ti_3C_2), hydrochloric acid 37% (HCl), acetonitrile ≥99.5% (C_2H_3N), triethanolamine ≥99% (TEOA), Urea≥99.5% ($CH4N_2O$), Calcium cyanide $Ca(CN)_2$ ≥99.9%, bipyridine ≥99% ($C_{10}H_8N_2$), hydrofluoric acid 48% (HF), chloroplatinic acid hexahydrate ≥99.9% ($H_2PtCl_6{\cdot}6H_2O$), and hydrogen peroxide 30% (H_2O_2), all obtained in high analytical quality, with distilled water.

Preparation of g-C_3N_4/$Ca(OH)_2$/Ti_3C_2

Ti_3C_2 MXene was synthesized by etching 2 g of Ti_3AlC_2 in 300 mL of 40% HF for 48 h, followed by centrifugation and vacuum drying at 60°C. The g-C_3N_4 (CN) was obtained by pyrolyzing 20 g of urea at 550°C for 3 h with a 5°C/min rate. The CN/CH-2/TC was synthesized by grinding 500 mg CN, 50 mg TC, and 30 mg $Ca(CN)_2$ in water, followed by heating at 350°C for 2 h in nitrogen. The heterostructures CN/CH-X/TC (X = 1, 2, 3) were prepared by varying $Ca(CN)_2$ amounts (0.015, 0.030, 0.045 g).

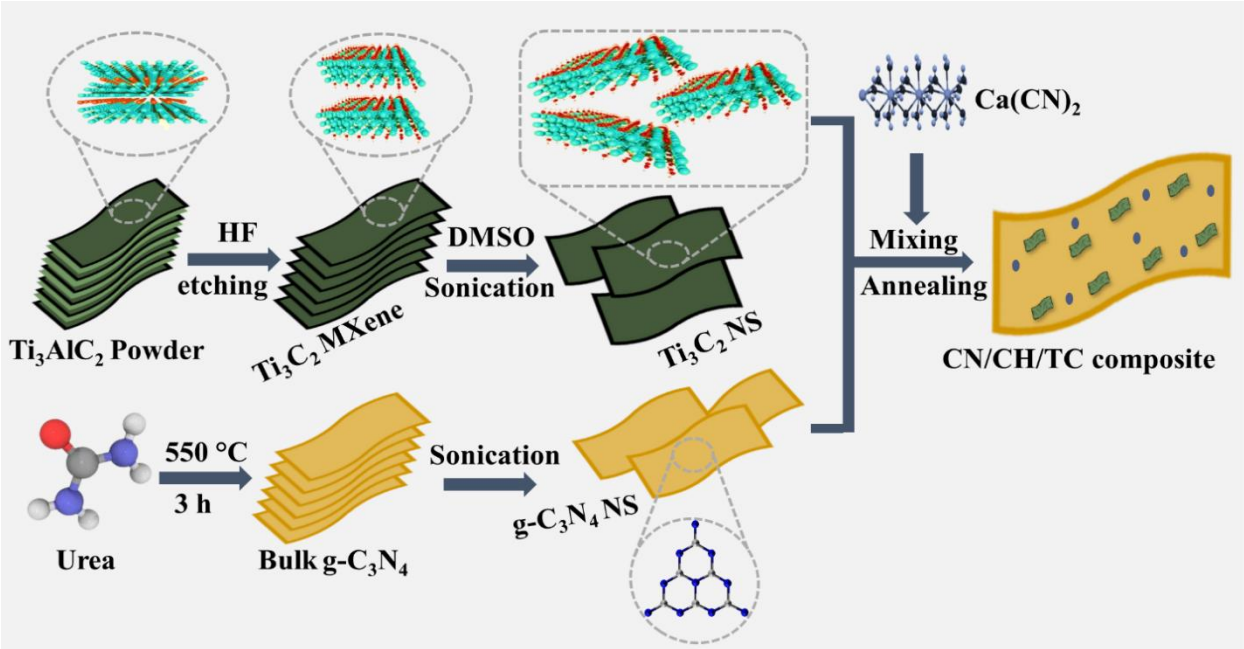

Scheme S1. The diagram illustrates the synthesis process of the CN/CH/TC composite.

Characterizations

The crystal structure of the samples was determined using XRD with copper anode X-ray emission (λ = 1.5406 Å), while BET surface area and porosity were evaluated with a Micromeritics ASAP 2460 analyzer. FTIR analysis with a TENSOR27 spectrometer, XPS measurements on an ESCALAB spectrometer, and

morphological studies using SEM (Hitachi S-4800), TEM, and HRTEM (Tecnai G2 F30S-Twin, FEI) were conducted. Optical properties were measured with a UV-visible spectrophotometer (PERSEE TU-1901), and electrochemical analysis was performed with a CHI760E electrochemical workstation.

Electrochemical Testing

The electrochemical workstation was used to conduct photocurrent measurements over time, EIS analysis, and Mott-Schottky tests. The three-electrode setup employed an electrically rectangular glass tape as the substrate. The conductive glass, coated over a 1 cm × 1 cm area and air-dried, acted as the working electrode in a 0.2 M Na_2SO_4 solution for electrochemical analysis. The coating suspension was obtained by sonicating 4 mg of the sample with 800 µL of water, 200 µL of absolute ethanol, and 50 µL of Nafion. EIS measurements were conducted by applying a 5 mV voltage across a frequency range of 0.1 to 10^5 Hz. The Mott-Schottky test was conducted at frequencies of 50 Hz and 100 Hz, covering a voltage interval from -0.3 V to 0.3 V. All electrochemical tests were performed using a three-electrode setup, with time-dependent current response measured under a 300 W xenon lamp cycling every 20 seconds.

Photocatalytic Activity Test

The photocatalytic H_2 evolution test used a sealed Pyrex system with overhead irradiation. A 50 mL mixture of 20 mg sample, 40 mL water, and 10 mL triethanolamine was sonicated for 10 minutes, with 3% Pt added in situ. After vacuum degassing for 30 minutes, a 300 W xenon lamp provided irradiation, and H_2 output was measured by gas chromatography using argon gas cooled at 6 °C. Photocatalytic CO_2 reduction was carriedout in a sealed Pyrex quartz reactor illuminated by a 300 W xenon lamp. A 20 mg sample was mixed with 6 mL TEOA, 12 mL water, and 45 mg bipyridine. The reactor, holding 18 mL MeCN and 3 mg $CoCl_2$, was sealed with silica glass. Air was evacuated, CO_2 was introduced to 0.08 MPa and dispersed for 30 minutes. The reaction proceeded at 15 °C, and products were analyzed chromatographically using argon as the carrier gas.

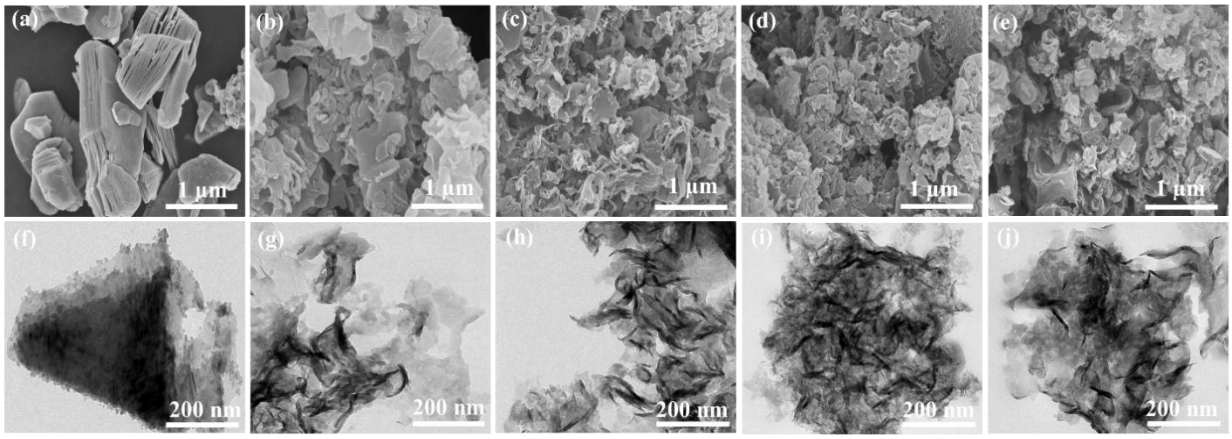

Fig. S1. FESEM and TEM images of (a, f) Ti_3C_2, (b, g) g-C_3N_4, (c, h) CN/TC, (d, i) CN/CH-1/TC and (e, j) CN/CH-3/TC.

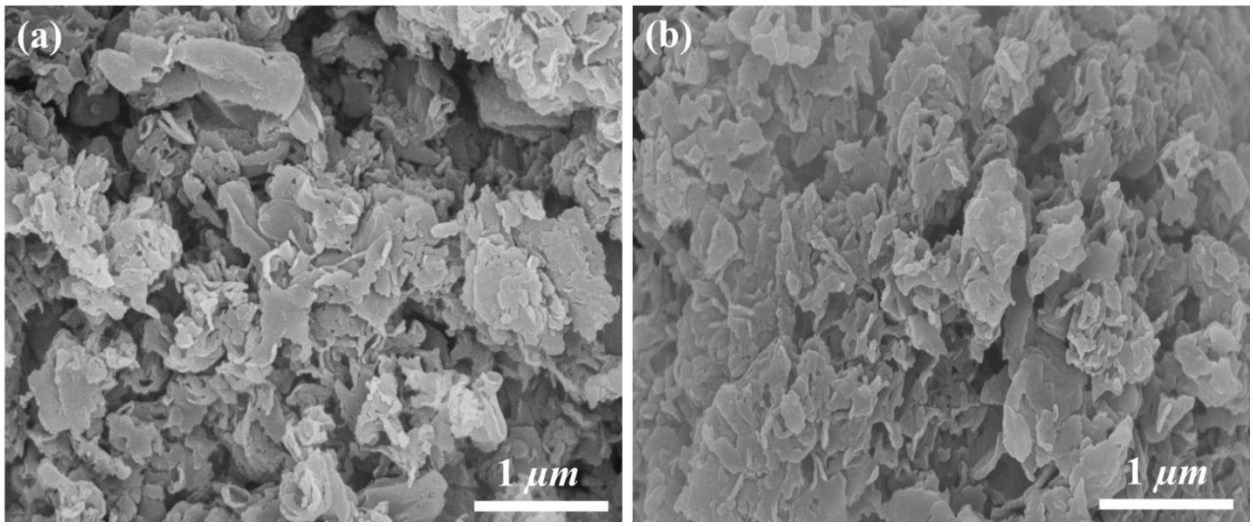

Fig. S2. FESEM (a) before recyclability, and (b) after recyclability.

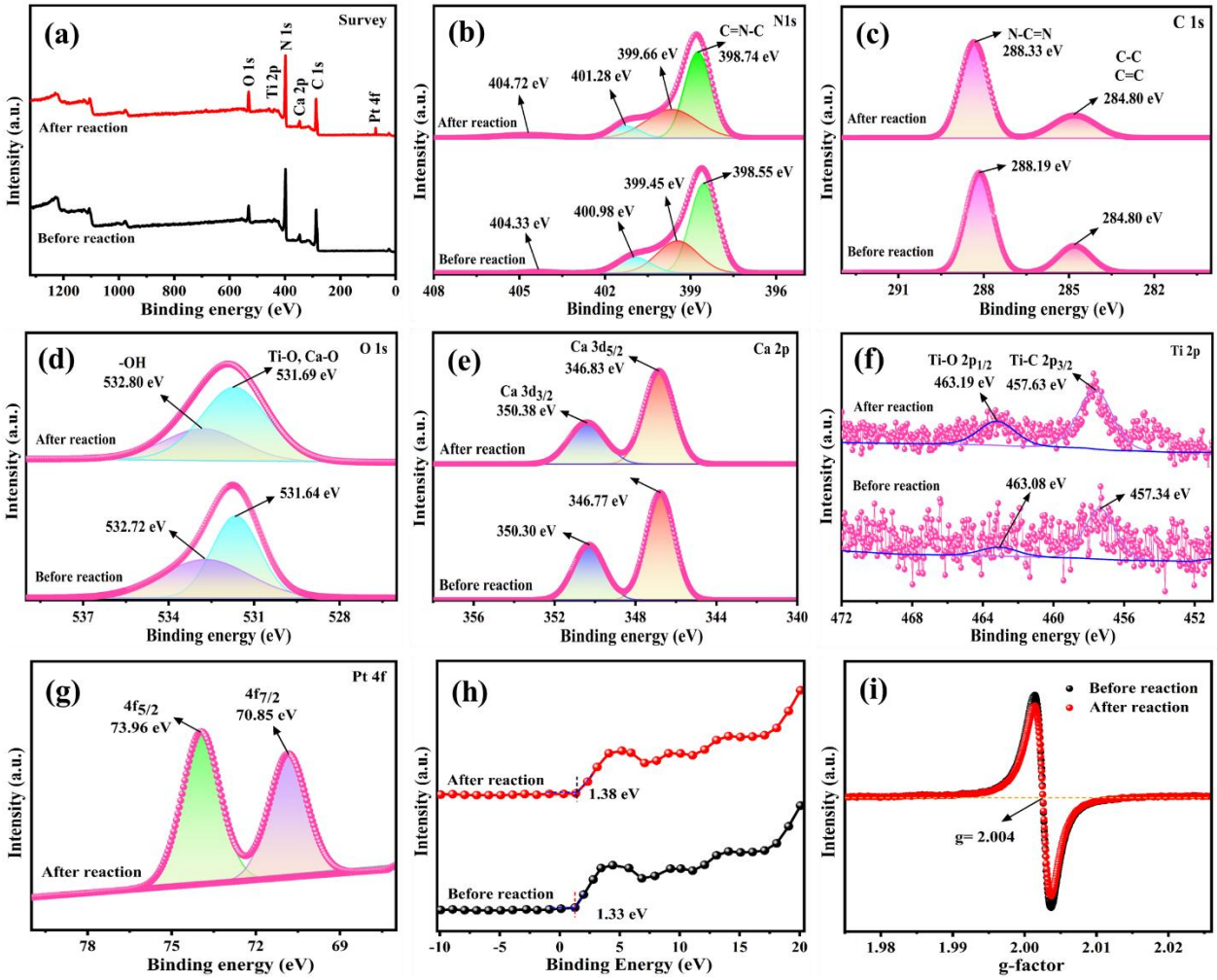

Fig. S3. XPS (a-h) and EPR (i) spectra before and after recyclability

Table S1

XPS N1s spectra deconvolution peak results of g-C_3N_4 and CN/CH-2/TC

Sample	g-C_3N_4			CN/CH-2/TC		
	N_{2C} C=N-C	N_{3C} N-$(C)_3$	N_{CH} C-N-H	N_{2C} C=N-C	N_{3C} N-$(C)_3$	N_{CH} C-N-H
Peak/eV	398.63	399.62	401.10	398.55	399.45	400.98
Area	36867.3	12774.7	8224.7	23885.4	19745.4	5310.2
Peak Ratio N_{2C}/N_{3C}	1.86			1.20		
Peak Ratio N_{CH}/N_{3C}	0.64			0.26		

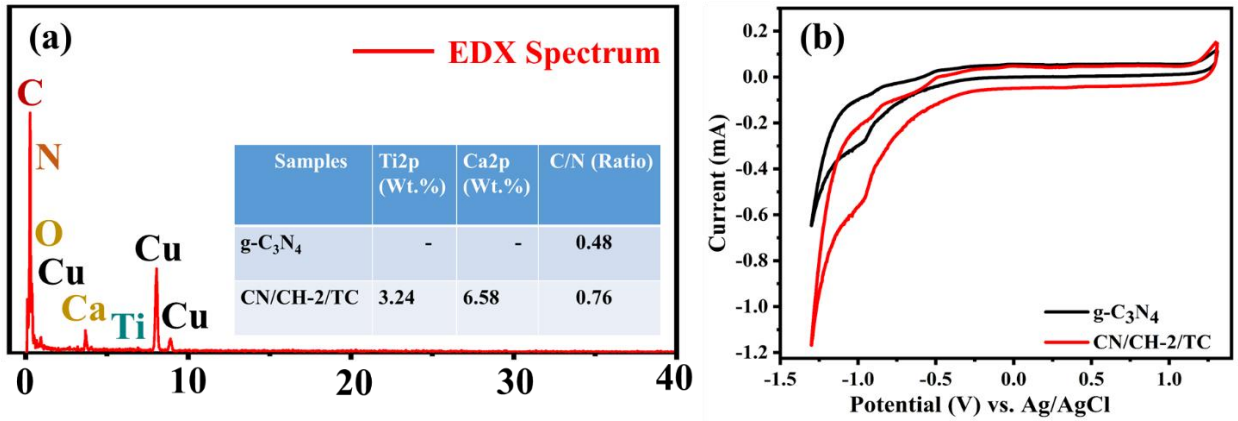

Fig. S4. (a) EdX of CN/CH-2/TC (b) CV analysis of g-C_3N_4 and CN/CH-2/TC.

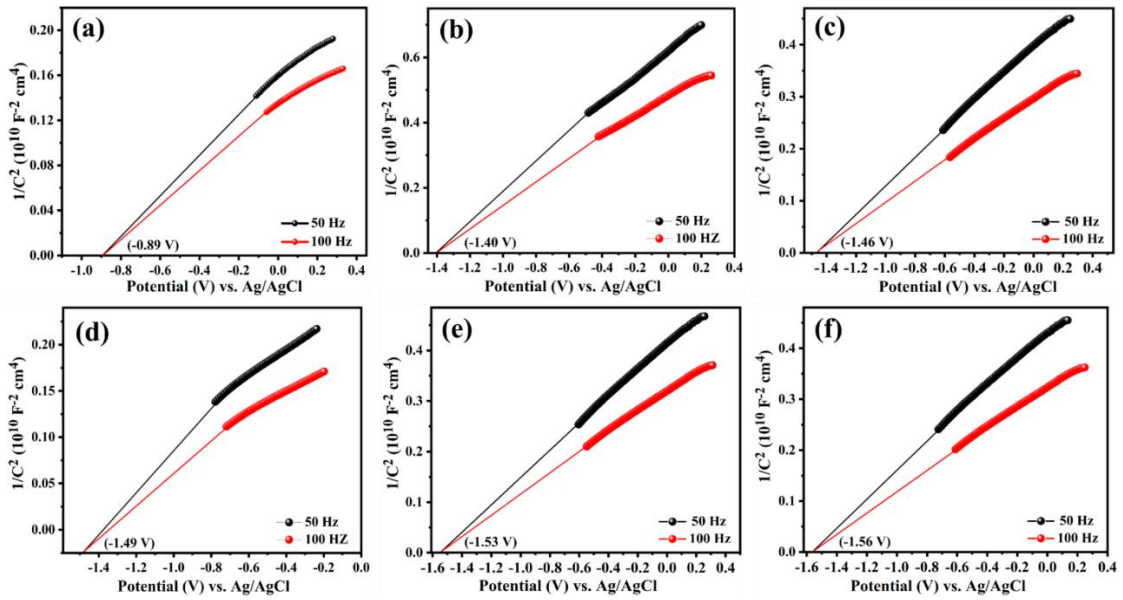

Fig. S5. Mott Schottky graphs of (a) Ti_3C_2, (b) g-C_3N_4, (c) CN/TC, (e) CN/CH-1/TC (e) CN/CH-2/TC, (f) CN/CH-3/TC.

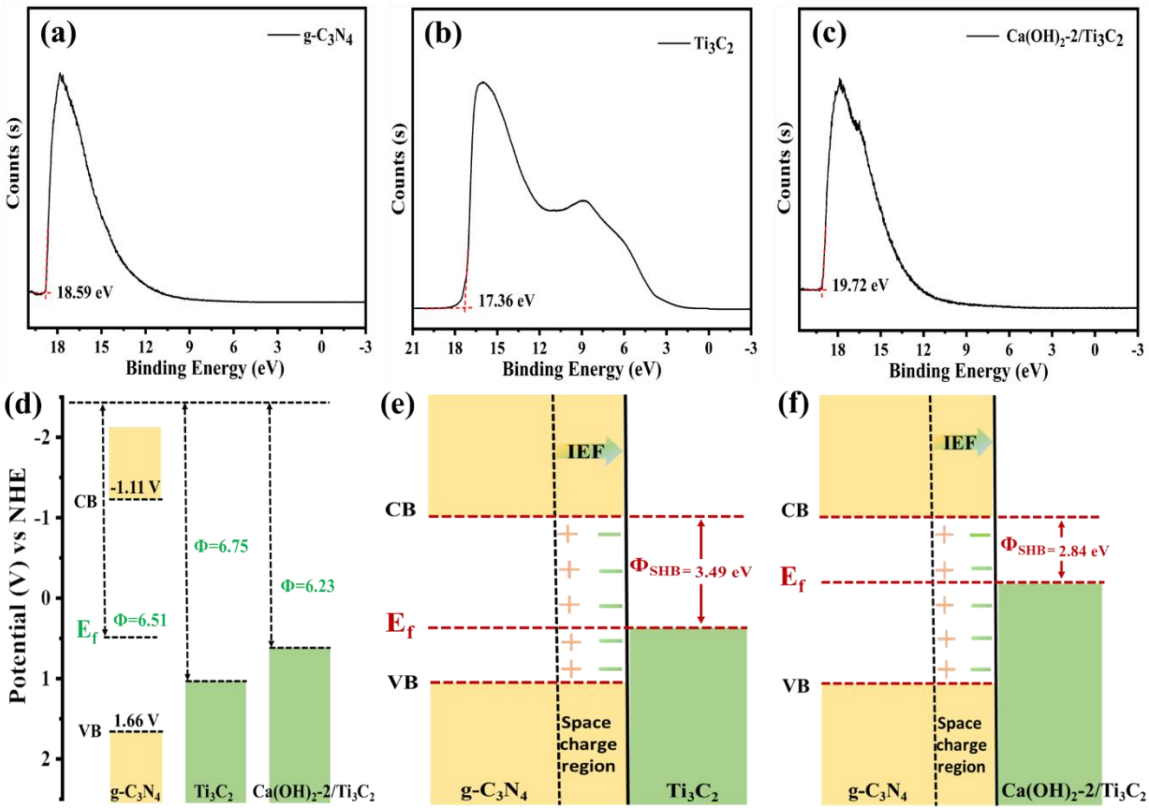

Fig. S6. UPS spectra of (a) g-C_3N_4, (b) Ti_3C_2, (c) $Ca(OH)_2$-2/Ti_3C_2, (d) band structure of g-C_3N_4, Ti_3C_2 and $Ca(OH)_2$-2/Ti_3C_2, and (h-i) Schematic illustrates SBH engineering showcasing improved electron flow and reduced recombination.

Table S2. Comparison of elemental composition (XPS), surface area (BET), and photophysical properties (TRPL) of bulk g-C_3N_4 and CN/CH-2/TC.

Sample	Carbon (wt.%)	Nitrogen (wt.%)	Oxygen (wt.%)	Ti 2p (wt.%)	Ca2p (wt.%)	C/N (atomic ratio)	S_{BET} (m^2/g)	Pore Volume (cm^3/g)	τ_a (ns)
Bulk g-C_3N_4	29.21	71.1	1.63	-	-	0.48	42	0.25	3.861
CN/CH-2/TC	30.2	46.14	13.83	3.24	6.58	0.76	134	0.58	5.217

Table S3. Comparison of photocatalytic H_2 evolution, CO_2 reduction of the typical materials reported in the past and our prepared material.

Samples	Catalyst Amount	Reactant Solution	H_2 Production	CO Production	Ref.
Mo-Mo_2C/g-C_3N_4	50 mg	20 vol.% TEOA/H_2O 3 % Pt	11291 μmol g^{-1} h^{-1}	-	1
PTCN/TC-2	30 mg	20 vol.% methanol	565 μmol g^{-1} h^{-1}	-	2
g-C_3N_4/Ti_3C_2	50 mg	10 vol.% TEOA/H_2O	116.2 μmol g^{-1} h^{-1}	-	3
g-C_3N_4/p-Ti_3C_2	50 mg	10 vol.% TEOA/H_2O	17.8 μmol g^{-1} h^{-1}	-	4
g-C_3N_4/Ti_3C_2	20 mg	10 vol.% TEOA/H_2O	727 μmol g^{-1} h^{-1}	-	5
Ti_3C_2/ g-C_3N_4	30 mg	10 vol.% TEOA/H_2O 3 % Pt	72.2 μmol g^{-1} h^{-1}	-	6
Ti_3C_2/g-C_3N_4	5 mg	10 vol.% TEOA/H_2O	26.7 μmolg^{-1} h^{-1}	-	7
Ti_3C_2/g-C_3N_4	40 mg	NaOH solution (1M)	-	CO: 11.21 μmol g^{-1} h^{-1}	8
gC_3N_4/ZnO/Ti_3C_2	10 mg	0.02 Mpa 3 ml H_2O	-	CO: 6.41 μmol g^{-1} h^{-1}	9
Ti_3C_2/g-C_3N_4	20 mg	3ml H_2O $NaHCO_3$ and concentrated H_2SO_4	-	CO : 5.19 μmol g^{-1} h^{-1}	10
g-C_3N_4/$BiOIO_3$ /Ti_3C_2	50 mg	NaOH solution (1M)	-	CO :5.88 μmol g^{-1} h^{-1}	11
TiO_2/g-C_3N_4/Ti_3C_2	100 mg	0.02 Mpa 3 ml H_2O	-	CO: 48.38 μmol g^{-1} h^{-1}	12
CN/CH-2/TC	**20 mg**	**10 vol.% TEOA/H_2O 3% Pt, MECN/TEOA=4:1**	**17300 μmol g^{-1} h^{-1}**	**CO=205.3 μmolg^{-1} h^{-1}**	**This Work**

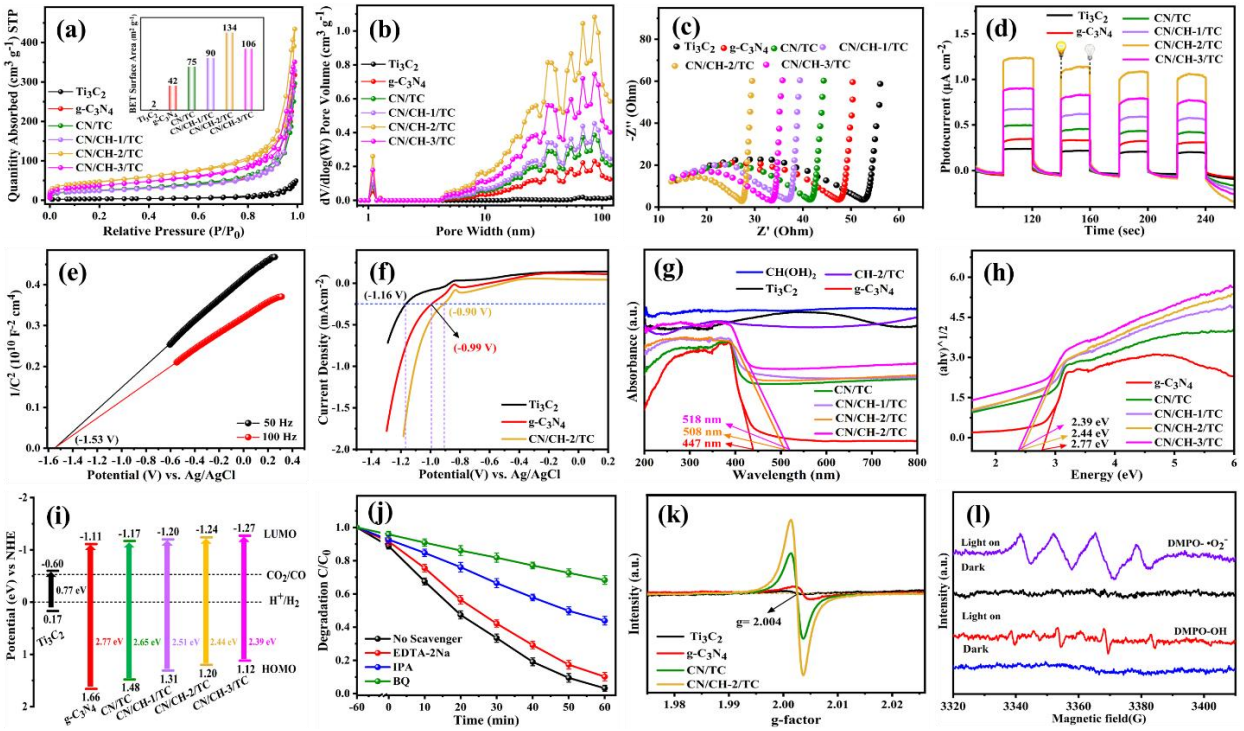

Fig. S7 BET measurement (a) isotherm plots of adsorption-desorption with inset S_{BET} (b) Ti_3C_2 pore diameter curves and CN/CH-X/TC (c) EIS spectra of Ti_3C_2 and CN/CH-X/TC (d) Photocurrent of Ti_3C_2 and CN/CH-X/TC (e) Mott Schottky plot CN/CH-2/TC (f) LSV spectra of Ti_3C_2, g-C_3N_4 and CN/CH-2/TC.

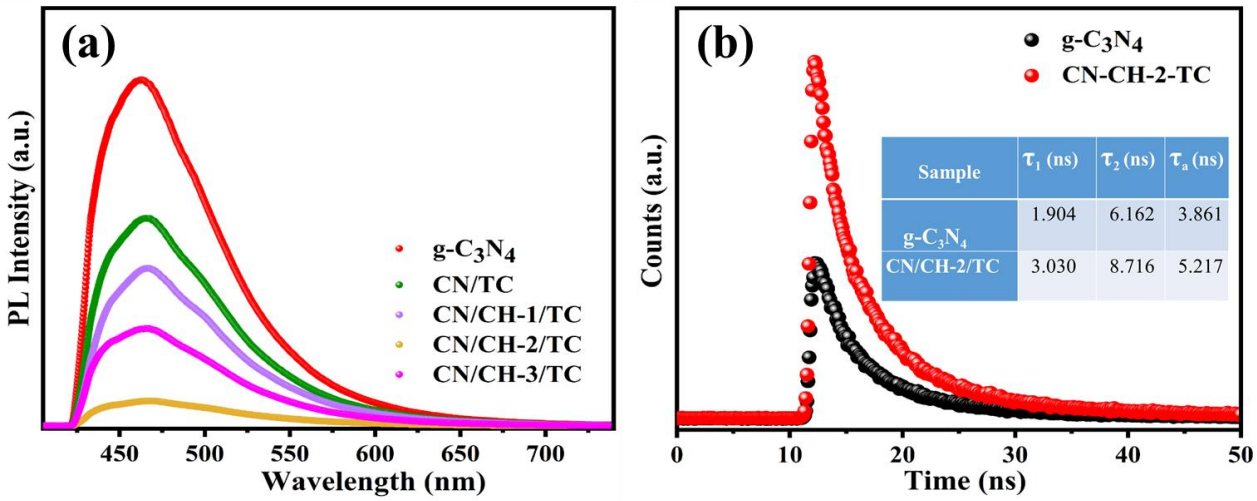

Fig. S8 (a) PL spectral data for the whole group of samples (b) TRPL of g-C_3N_4 and CN/CH-2/TC.

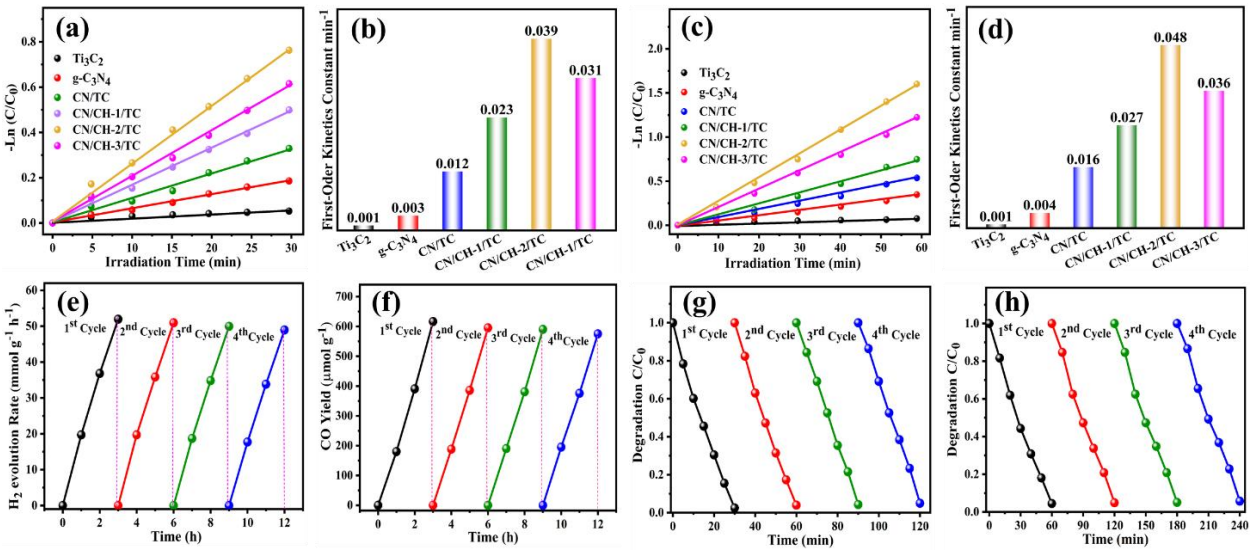

Fig. S9. (a, c) Photocatalytic degradation rate for methyle blue and tetracycline and (b, d) first-order kinetics constants for MB and TC (e) recyclability of CN/CH-2/TC for H_2 evolution (f) recyclability of CN/CH-2/TC for CO evolution (g) recyclability of MB (h) recyclability of TC.

Calculation method of quantum yield (QY) and apparent quantum efficiency (AQE)

QY for CO_2RR to CO refers to the ratio of the number of reacted electrons to the total number of absorbed photons and can be described as:

$$\mathrm{QY}\ (\%) = \frac{\text{Number of reacted electrons}}{\text{Number of absorbed photons}} \times 100\%$$
$$= \frac{\text{Number of evolved CO molecules} \times 2}{\text{Number of absorbed photons}} \times 100\%$$
$$= \frac{N_A \times n \times 2}{N} \times 100\%$$

Where, N_A stands for Avogadro's constant, n for the amount of substance of CO, and N for the number of incident photons. The number of absorbed photons is found by the wavelength, energy density, and area of the irradiation as follows:

$$N = \frac{P \times \lambda \times t}{h \times c} \times A$$

$$\mathrm{AQE}(\%) = \frac{\text{Number of reacted electrons}}{\text{Number of incident photos}} \times 100\%$$
$$= \frac{\text{Number of evolved CO molecules} \times 2}{\text{Number of incident photos}} \times 100\%$$
$$= \frac{N_A \times n \times 2}{N} \times 100\%$$

Where, N_A stands for Avogadro's constant, n for the amount of substance of CO, and N for the number of incident photons. The number of incident photons is found by the wavelength, energy density, and area of the irradiation as follows:

$$N = \frac{P \times \lambda \times t}{h \times c}$$

Where P stands for optical power, λ for the wavelength of the incident photon, t for the irradiation time, h for Planck's constant, c for the speed of light, and A absorbance efficiency.

Table S4. Quantum yield (QY) and apparent quantum efficiency (AQE)

Wavelength (nm)	CO (μmol)	Absorbance (A)	QY (%)	AQE (%)
420	26.1	0.81	11.4	9.2
550	22.7	0.74	6.9	5.1
650	17.3	0.69	4.4	3.1

Photocatalytic mechanism

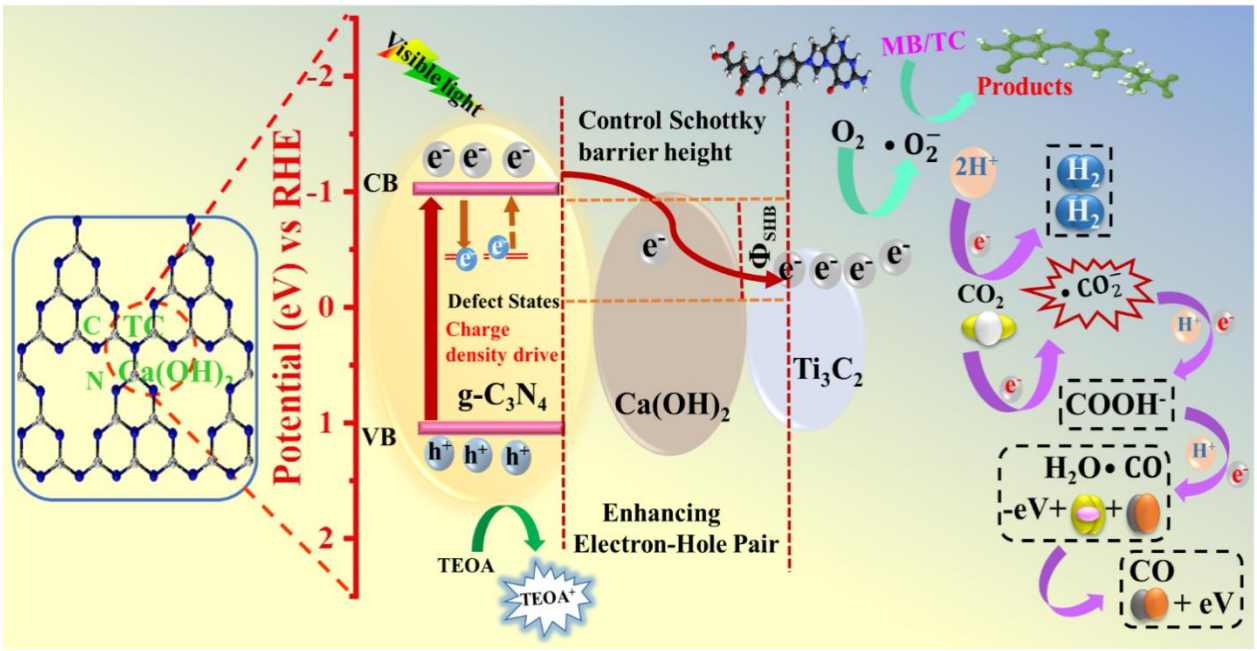

Fig. S10. A schematic diagram illustrates the photocatalytic mechanism.

References

1. Y. Zheng, J. Dong, C. Huang, L. Xia, Q. Wu, Q. Xu and W. Yao, Appl Catal B: Environ, 2020, **260**, 118220.
2. K. Huang, C. Li, X. Zhang, L. Wang, W. Wang and X. Meng, Green Energy Environ, 2023, **8**, 233-245.
3. J. Li, L. Zhao, S. Wang, J. Li, G. Wang and J. Wang, Appl Surf Sci, 2020, **515**, 145922.
4. F. Xu, D. Zhang, Y. Liao, G. Wang, X. Shi, H. Zhang and Q. Xiang, J Am Ceram Soc, 2020, **103**, 849-858.
5. H. Xu, R. Xiao, J. Huang, Y. Jiang, C. Zhao and X. Yang, Chinese J Catal, 2021, **42**, 107-114.
6. T. Su, Z. D. Hood, M. Naguib, L. Bai, S. Luo, C. M. Rouleau, I. N. Ivanov, H. Ji, Z. Qin and Z. Wu, Nanoscale, 2019, **11**, 8138-8149.
7. H. Dong, X. Zhang, Y. Zuo, N. Song, X. Xin, B. Zheng, J. Sun, G. Chen and C. Li, Appl Catal A 2020, **590**, 117367.
8. Q. Tang, Z. Sun, S. Deng, H. Wang and Z. Wu, J colloid Interf Sci, 2020, **564**, 406-417.
9. J. Li, Y. Wang, Y. Wang, Y. Guo, S. Zhang, H. Song, X. Li, Q. Gao, W. Shang and S. Hu, Nano Mater Sci, 2023, **5**, 237-245.
10. C. Yang, Q. Tan, Q. Li, J. Zhou, J. Fan, B. Li, J. Sun and K. Lv, Appl Catal B: Environ, 2020, **268**, 118738.
11. L.f. Hong, R.t. Guo, Y. Yuan, X.y. Ji, Z.d. Lin, X.f. Yin and W.g. Pan, Colloids Surf A, 2022, **639**, 128358.
12. A. A. Khan, M. Tahir and A. Bafaqeer, Energy Fuels, 2020, **34**, 9810-9828.